Performance and durability of broadband antireflection coatings for thin film CdTe solar cellsa)

Gerald Womack, Piotr M. Kaminski, Ali Abbas, Kenan Isbilir, Ralph Gottschalg, and John Michael Walls

Citation: J. Vac. Sci. Technol. A **35**, 021201 (2017); doi: 10.1116/1.4973909

View online: http://dx.doi.org/10.1116/1.4973909

View Table of Contents: http://avs.scitation.org/toc/jva/35/2

Published by the American Vacuum Society

Performance and durability of broadband antireflection coatings for thin film CdTe solar cells[a)]

Gerald Womack, Piotr M. Kaminski, Ali Abbas, Kenan Isbilir, Ralph Gottschalg, and John Michael Walls[b)]
Centre for Renewable Energy Systems Technology, (CREST), Wolfson School of Mechanical, Electrical and Manufacturing Engineering, Loughborough University, Loughborough, Leicestershire LE11 3TU, United Kingdom

(Received 5 September 2016; accepted 21 December 2016; published 13 January 2017)

Light reflection from the glass surface of a photovoltaic (PV) module is a significant source of energy loss for all types of PV devices. The reflection at the glass and air interface accounts for ~4% of the total energy. Single layer antireflection coatings with sufficiently low refractive index have been used, such as those using magnesium fluoride or porous silica, but these are only effective over a narrow range of wavelengths. In this paper, the authors report on the design, deposition, and testing of multilayer broadband antireflection coatings. These coatings reduce the weighted average reflection over the wavelength range used by thin film CdTe devices to just ~1.22%, resulting in a 3.6% relative increase in device efficiency. The authors have used multilayer stacks consisting of silica and zirconia layers deposited using reactive magnetron sputtering. Details of the stack design, sputter deposition process parameters, and the optical and microstructural properties of the layers are provided. Antireflection coatings on glass exposed to the outdoors must not degrade over the lifetime of the module. A comprehensive set of accelerated environmental durability tests has been carried out in accordance with IEC 61646 PV qualification tests. The durability tests confirmed no damage to the coatings or performance drop as a result of thermal cycling or damp heat. All attempts to perform pull tests resulted in either adhesive or substrate failure, with no damage to the coating itself. The coatings also passed acid attack tests. Scratch resistance, abrasion resistance, and adhesion tests have also been conducted. The optical performance of the coatings was monitored during these tests, and the coatings were visually inspected for any sign of mechanical failure. These tests provide confidence that broadband antireflection coatings are highly durable and will maintain their performance over the lifetime of the solar module. All dielectric metal-oxide multilayer coatings have better optical performance and superior durability compared with alternative single layer porous sol–gel coatings. Thin film CdTe devices are particularly problematic because the antireflection coating is applied to one side of the glass, while device layers are deposited directly on to the opposite glass surface in the superstrate configuration. In thin film CdTe production, the glass is exposed to high temperature processes during the absorber deposition and the cadmium chloride activation treatment. If glass precoated with a broadband antireflection coating is to be used, then the coating must withstand temperatures of up to ~550 °C. Surprisingly, our studies have shown that multilayer silica/zirconia antireflection coatings on soda lime glass remain unaffected by temperatures reaching 600 °C, at which point mild crazing is observed. This is an important observation, demonstrating that low cost glass, which is preprocessed with a broadband antireflection coating, is directly useable in thin film CdTe module production. [http://dx.doi.org/10.1116/1.4973909]

I. INTRODUCTION

Antireflection coatings are used in conjunction with photovoltaic (PV) devices to reduce reflection from the air–glass interface. Commercial coatings for solar modules must be durable on a time-scale comparable to the industry standard for solar modules, which are normally provided with a 25 year warranty. Any solar cell technology must undergo rigorous testing to ensure that solar modules can endure decades of outdoor exposure. Antireflection coatings applied to solar modules must have equivalent durability.

A variety of tests are available to assess the durability of surface coatings. For example, nanoindentation scratch tests can be used to measure the scratch resistance of a coating,[1] whereas the pull test and crosshatch test are useful to evaluate the adhesion of the coating. Additionally, in the case of precoated glass, resistance to the high temperatures involved in the solar cell deposition is necessary.[2] A coating resistant to all forms of mechanical and environmental damage can be considered durable. Resistance to weathering damage associated with using the solar module outdoors in the field can be determined using tests such as damp heat (DH),[3] cyclic humidity,[3] and acid attack.[4] Acceptable durability is considered to be the ability of the coating to withstand exposure to subsequent module manufacturing processes, long term environmental exposure, and operational maintenance work.

[a)]Paper presented at the 62nd AVS International Symposium, San Jose, November 2015.
[b)]Electronic mail: j.m.walls@lboro.ac.uk

Single layer antireflection (AR) coatings using magnesium fluoride (MgF_2), or porous silica with sufficiently low refractive index, have been used on solar cells and solar modules. However, these coatings are only effective over a relatively narrow wavelength range. Additionally, as MgF_2 is hydrophilic, it has poor durability to weathering and is therefore unsuitable for outside use and has been used only to increase light transmission into champion devices.[5] Porous silica coatings, normally deposited by sol–gel deposition methods, integrate air pockets into the coating to lower the overall refractive index. This results in reduced scratch-resistance and coating hardness.[6] Commercial porous sol–gel coatings use resins to improve adhesion. However, the improvements made for adhesion and scratch-resistance may compromise the optical properties. These more mechanically stable sol–gel coatings have reduced antireflection properties when compared to basic porous silica, as their complex porous/netlike structure increases light scattering and absorption due to increased density.[6]

We report on the design and durability of broadband antireflection coatings consisting of all dielectric multilayers of metal-oxides. We have investigated the performance, durability, heat resistance, microstructure, and adhesion of silica/zirconia multilayer antireflection coatings (MAR), deposited using reactive magnetron sputtering. Some details of the stack design, sputtering process parameters, and the optical and microstructural properties of the layers have been provided previously,[7] but further details are provided here.

MAR coatings avoid the mechanical issues that arise from reducing the packing density of a material because a layer with a very low refractive index is not required. Metal-oxide dielectric coatings also have high hardness coefficients and very low extinction coefficients. MAR coatings manipulate the reflections from different layers within the coating to create destructive reflective interference, thereby increasing the transmission of light into the cell. MAR coatings are versatile and can be optimized for use over specific wavelength ranges. Consequently, MAR coatings of varying designs have been optimized for use on thin film CdTe solar cells,[7] perovskites,[8] amorphous silicon,[8] crystalline silicon,[9] and copper indium gallium di-selenide (CIGS).[10]

II. THIN FILM CDTE PHOTOVOLTAIC DEVICES

Thin film CdTe PV technology is an attractive alternative to the dominant crystalline silicon (c-Si) based PV due to its low manufacturing costs. Recently, significant progress has been made in the device technology. First Solar, Inc., has reported 22.1% cell and 18.6% module level conversion efficiencies.[11,12] The reported efficiencies were the result of a continuous industrial development. This rapid progress has been made after the record efficiency stagnated at 16.5% for 10 years (2001–2011).

CdTe is a II–IV semiconductor material with a band gap of $\sim$1.45 eV. A 2 μm thick absorber is typically used for solar cell fabrication. Thin film CdTe used in devices is a polycrystalline material and can be deposited by a number of techniques, including electrodeposition, evaporation, close space sublimation (CSS), vapor transport deposition (VTD), and magnetron sputtering.[13–16] VTD is currently the most commonly used industrial technique for thin film CdTe PV manufacturing and was used for the record cell and module fabrication. The deposition of the semiconductor is carried out at temperatures that range from 200 °C for magnetron sputtering to 550 °C (Ref. 17) for techniques such as CSS and VTD.[18,19]

Thin film CdTe solar modules are deposited in the superstrate configuration on float glass coated with a transparent conducting oxide such as NSG-Pilkington TEC glass. TEC glass is coated with fluorine doped tin oxide. It is available in a variety of thickness options, offering different levels of transmittance and conductivity to accommodate different types of PV absorbers. A typical thin film CdTe device consists of a CdS/CdTe heterojunction as shown in the simple configuration in Fig. 1. The CdS acts as an n-type window layer and is necessary to form the p-n junction.

III. BROADBAND MULTILAYER ANTIREFLECTION COATINGS: DESIGN AND FABRICATION

Thin film CdTe PV modules experience reflection losses due to the difference between the refractive index of the glass superstrate and the air. The front surface reflections are responsible for losses of over 4% of the incident light. The reflection losses can be reduced by the application of an AR coating. The simplest option is to deposit a single layer refractive index, matching AR with a material with a low refractive index. MgF_2 has a low refractive index ($n = 1.34$ at 550 nm).[20] A thin film of MgF_2 provides an effective AR coating over a narrow range of wavelengths. However, MgF_2 is a soft material and suitable for laboratory use only. Porous silica is another single layer option, although long-term stability can be an issue for this type of coating due to potential problems with water ingress.[21] MAR coating is a more complex design but effective over a broader wavelength range. The design of a MAR coating is based on high/low refractive index material pairs and does not require a material with a refractive index lower than glass.

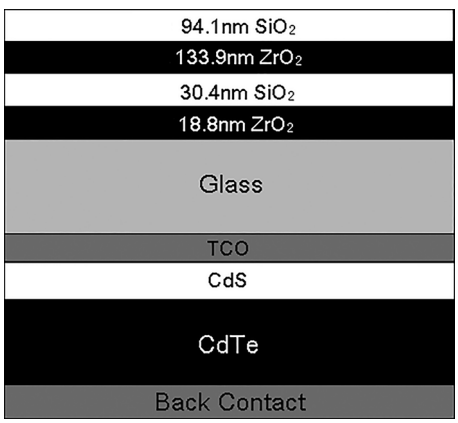

FIG. 1. Schematic diagram of the MAR coating design on a CdTe device, the refractive index of the glass superstrate is $n = 1.51$ at 550 nm.

A. Coating design principles

The design of a broadband antireflection coating uses a combination of materials with low and high refractive index. The low index material used is almost always thin film silicon dioxide (SiO_2) with a refractive index of ~1.46 at 550 nm. A wide choice of materials is available for the high index thin films and these are listed in Table I together with their important optical and mechanical properties. The choice of high index material depends on the application, but is often a compromise between optical properties, durability, and cost. For applications on solar modules, the durability is a key consideration. For this reason, we have chosen to use zirconium dioxide (ZrO_2) which has exceptional scratch resistance and is relatively abundant and low cost. Titanium dioxide (TiO_2) is another economically viable option.

The MAR coating requires accurate control of each layer thickness to maximize destructive interference and minimize the overall reflection. The coatings are designed using optical constants derived from spectroscopic ellipsometry measurements. The MAR coatings are designed to minimize average reflection over the specific spectral range corresponding to the PV absorber band gap. In the case of a CdTe absorber, the band gap is ~1.45 eV, which corresponds to a wavelength of ~855 nm, but CdTe begins to absorb light less efficiently as it approaches this limit. As glass begins to absorb at 350 nm, this means that the wavelength range used by CdTe devices is between350 and 850 nm. In comparison, a single layer design optimizes at a single wavelength to create a "V-coat" AR. MAR coatings are broadband and their use results in a much greater reduction in average reflection. The bandwidth can be tuned for the different band gaps used in various PV absorbers by controlling the thickness of the layers within the MAR coating.[8]

The coating layer thicknesses were optimized to reduce reflection using the optical modeling package "Essential Macleod" developed by the Thin Film Center, Inc.[31] This package uses the transfer matrix method to calculate transmittance and reflectance in optical coating systems. The transfer matrix method allows an optical system that is a sum of optical matrices to be considered as a single matrix, a "transfer matrix" as defined in Eq. (1). The transfer matrix (S) equals the multiplication of interface (I) and layer (L) matrices, of layer integer $\leq n$, multiplied by the interface matrix of the boundary between the last and penultimate materials in the system. This method has been shown to be accurate when modeling light through multilayer systems with distinct boundaries between layers[9,32]

$$S = \left(\prod_{n=1}^{m} I_{(n-1)n} L_n \right) \cdot I_{m(m+1)}. \tag{1}$$

The thickness of each layer in the four layer design was optimized to lower the weighted average reflection (WAR) from the glass–air interface. A WAR is the weighted average of reflection of all solar photons across the wavelength range of interest. To calculate accurately the WAR from bare glass and MAR coated glass, the relative flux of photons in the solar spectrum at each point in the 350–850 nm range must be taken into consideration and the wavelengths given appropriate weightings.[8] The WAR is described by Eq. (2), which shows the product of the AM1.5G solar spectrum (Φ) and the reflectance (R), integrated over the defined wavelength range (λ)

$$\mathrm{WAR}(\lambda_{\max}, \lambda_{\min}) = \int_{\lambda_{\min}}^{\lambda_{\max}} \frac{\Phi \cdot R}{R} d\lambda. \tag{2}$$

B. Coating design for thin film CdTe photovoltaics

MAR coatings vary in the number of layers used. The addition of extra layers when designing MAR coatings results in lower reflection, but in terms of reflection reduction, the difference between a six layer and a four layer design is much less than the difference between a four layer and a two layer design. Evaluating the benefits of greater reduction in reflection against the greater material costs and increased coating complexity, a four layer design was considered optimum for the 350–850 nm wavelength range. Figure 1 shows the detailed structure of the MAR design on top of a simple CdTe PV stack. Optical interference does occur in the thin film CdTe device, but its effect on the MAR coating design is minimal. MAR coating designs are not unique and a number of possible solutions are possible. This design leads to a relatively thin multilayer stack (~277 nm), which is affordable in materials usage and fabrication time.

C. Performance with angle of incidence

The angle at which light enters a solar cell will vary depending on the position of the sun. As a result of the sun's changing position in the sky and diffuse conditions such as

TABLE I. Optical constants and important mechanical properties of candidate high index materials for use in MAR coatings.

Material	Coefficient of thermal expansion (10^{-6}/C)	Hardness–Vickers (GPa)	Refractive index (n) at 550 nm	Extinction Coefficient (k) at 550 nm
Silicon dioxide (SiO_2)	0.4 (Ref. 22)	~12.4 (Ref. 23)	1.46	0
Zirconium dioxide (ZrO_2)	13.5 (Ref. 24)	~13.0 (Ref. 25)	2.23	0
Titanium dioxide-anatase (TiO_2-a)	8.6 (Ref. 26)	~11.0 (Ref. 23)	2.49	0
Titanium dioxide-rutile (TiO_2-r)	8.4 (Ref. 26)	~12.0 (Ref. 27)	2.61	0
Hafnium-oxide (HfO_2)	5.9 (Ref. 28)	~14.7 (Ref. 29)	1.93	0
Tantalum pentoxide (Ta_2O_5)	3.0 (Ref. 30)	~13.7 (Ref. 29)	2.15	0
Niobium pentoxide (Nb_2O_5)	~3.0 (similar to Ta_2O_5) (Ref. 30)	~15 (Ref. 28)	2.32	0

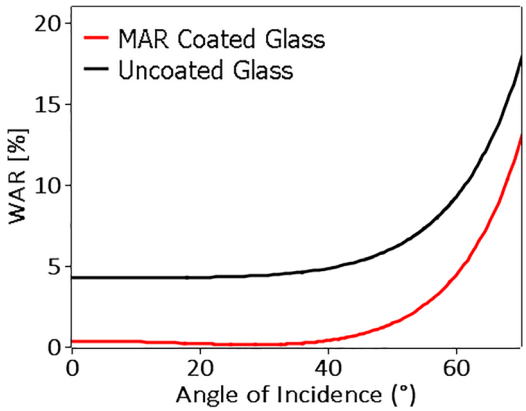

FIG. 2. (Color online) WAR modeled for the MAR coating design and compared with uncoated glass for a range of angles of incidence.

occurs in cloudy weather, the MAR coating must be functional over a broad range of angles of incidence. The MAR coating reduces reflection at all angles of incidence and is effective in both direct and in diffuse illumination. The effect of angle of incidence on WAR reflectance for the MAR coating design presented in Fig. 1 is shown in Fig. 2.

D. Multilayer antireflection coating deposition

Multilayer antireflection coatings can be deposited using a number of techniques including electron beam evaporation with ion assist,[33] ion beam sputtering,[33] and magnetron sputtering.[7] These are relatively high energy techniques that deposit compact thin films with refractive indices close to bulk values.

The MAR coatings were deposited by reactive magnetron sputtering using a "PV Solar" system from PowerVision, Ltd. A three-dimensional layout of the system is shown in Fig. 3. Prior to being loaded into the deposition chamber,

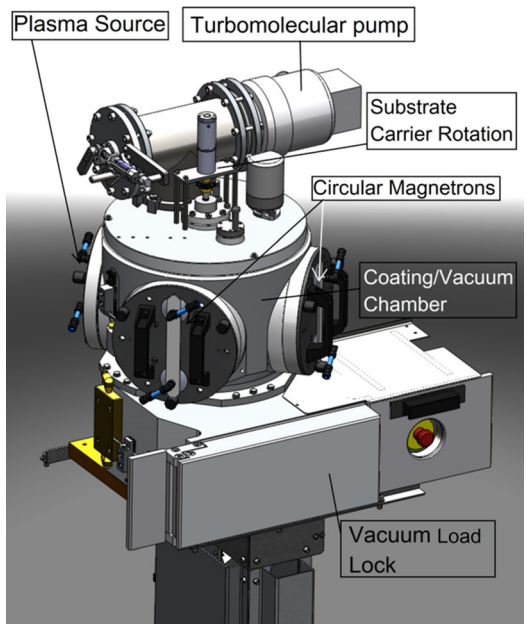

FIG. 3. (Color online) 3D schematic diagram of the reactive sputtering system used to deposit the MAR coatings.

soda lime glass substrates were cleaned in an ultrasonic bath in a 50%–50% solution of deionized water and isopropyl alcohol. After cleaning, the substrates were loaded into the deposition chamber via a load lock.

The system uses a vertical substrate carrier which rotates at ~120 rpm. The vacuum chamber is equipped with three vertically mounted 150 mm diameter circular magnetrons and a separate DC plasma source. The rotating carrier can accommodate up to six 5 × 5 cm glass substrates. Two of the magnetrons were fitted with zirconium metal and silicon planar targets. The deposition chamber is pumped using a turbomolecular pump (Edwards nEXT300D) mounted vertically, above the plasma source. The preprocess pressure is typically 1×10^{-5} mbar. Argon working gas is admitted in front of the magnetrons, and the pressure (2.5 mTorr) is controlled using mass flow controllers (MKS 1179A). Argon and oxygen gas flows into the plasma source were also controlled by mass flow controllers. During the SiO_2 deposition, the gas flow was set at 16 sccm (Ar) and 10 sccm (O_2). For the deposition of ZrO_2, the gas flow was set to 20 sccm (Ar) and 6 sccm (O_2). The operation of each magnetron and all process parameters are under computer control.

A 120 s argon/oxygen plasma pretreatment was used for surface activation. This pretreatment increases the substrate surface energy as determined by a water contact angle measurement. Surface activation improves adhesion. The argon flow to the plasma source was subsequently terminated to produce an oxygen plasma for oxidation of the zirconium and silicon layers. A thin layer of metal, typically ~1 nm thickness, is deposited in each pass of the rotating carrier, which is fully oxidized as it passes through the oxygen plasma to produce an optical quality oxide. High deposition rates can be achieved with this reactive sputtering strategy because the metal layer is deposited using a pulsed DC power supply (Advanced Energy, Inc., Pinnacle Plus 5 kW) and hysteresis effects are also avoided.[34–36] The frequency of the pulse was set to 150 kHz (6.6 μs per pulse) for both materials. The zirconium was sputtered at 1 kW using a 1.5 μs (~25% reverse time), while the silicon was deposited at 1.5 kW and 2.5 μs (~50% reverse time). The deposition rate was 0.67 nm/s for SiO_2 and 0.7 nm/s for ZrO_2 films at each position on the rotating substrate carrier. The metal deposition zone and the plasma oxidation zone are separated by internal baffles to avoid poisoning of the metal targets. Layer thickness is controlled using time only since the metal sputtering rate is highly stable. Quartz crystal monitoring is not required. The computer control is set to switch between the magnetrons for preselected times corresponding to each layer thickness required. Further details of the deposition system and the deposition parameters are available elsewhere.[7]

E. Coating microstructure

Samples for transmission electron microscopy (TEM) were prepared by focused ion beam (FIB) milling using a dual beam FEI Nova 600 Nanolab. An electron beam evaporated platinum (e-Pt) over-layer was deposited followed by an ion assisted layer to define the surface and homogenize

the final thinning of the samples down to ~100 nm. The TEM analysis was carried out using a Tecnai F20, operating at 200 kV to investigate the detailed microstructures of the MAR coating cross sections. Bright field STEM images were obtained, revealing the layer thicknesses, uniformity, and microstructure.

Figure 4 shows a STEM image of a cross section of the MAR coating produced by FIB. The image shows that the coating is dense and uniformly covers the surface. No voids or pinholes are observed. Voids would degrade the optical performance by affecting the refractive index. Film density is also critical for achieving the coating durability required for the PV application. The presence of voids or pinholes provides access for water ingress and leads to degradation. The excellent coating uniformity observed is crucial for achieving and maintaining AR performance across large area PV modules. The SiO_2 appears amorphous while the structure in the ZrO_2 is columnar and typical for a sputtered thin film.

IV. RESULTS AND DISCUSSION

A. Increase in photocurrent and efficiency

MAR coatings were deposited on the glass superstrate of thin film CdTe devices to confirm that the cell performance improvement corresponds to the optical modeling. The thin film CdTe devices used in this study were fabricated at Colorado State University using their advanced research deposition system.[13]

A four layer MAR coating corresponding to the design shown in Fig. 1 was deposited sequentially using reactive magnetron sputtering. The reflection from the uncoated glass surface and the MAR coated surface was measured using a UV-vis spectrophotometer (as shown in Fig. 5). The application of the MAR coating reduces the WAR of soda lime glass by 2.9% in absolute terms, corresponding to a relative reduction in reflection of 69%.[8] Reducing reflectance and increasing transmission at the glass surface results in greater cell efficiency, as shown in Fig. 6. Figure 6 shows the J-V characteristics of a thin film CdTe cell before and after application of the broadband antireflection coating. The

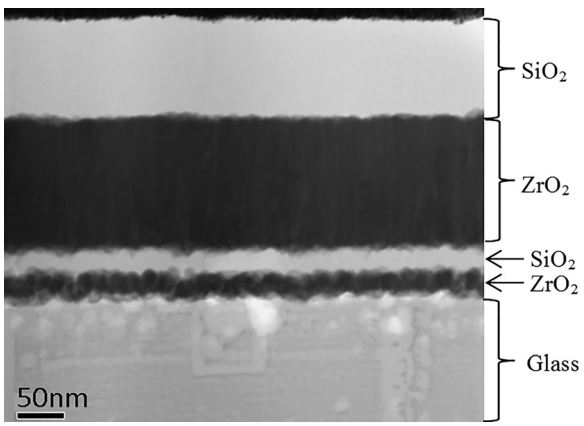

FIG. 4. STEM image of a cross-section of the MAR coating deposited using reactive sputtering. The SiO_2 is amorphous, and the ZrO_2 has a columnar structure.

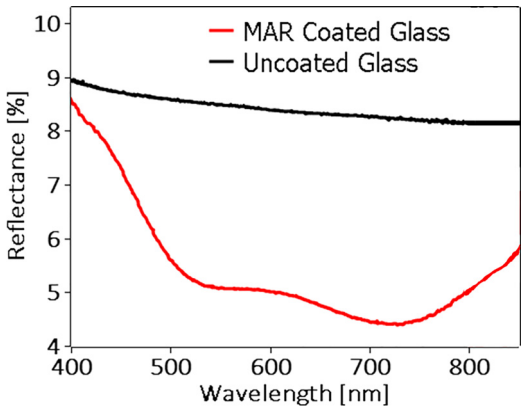

FIG. 5. (Color online) Measured reflectance of bare and MAR coated glass.

maximum short circuit current density was increased by 0.65 mA/cm^2 while the open-circuit voltage was unchanged. This increased the overall efficiency of the device from 10.6% to 10.9%, a useful relative increase of 3.6%. Table II summarizes the design and performance of the MAR coating designed for CdTe and its effect on short circuit current.

B. Durability of the multilayer antireflection coatings

1. Adhesion

Adhesion is an important factor for coatings on thin-film PV modules. Clearly high adhesion results in a coating with greater durability as the coating is harder to remove from the glass. Adhesion of the MAR coatings was measured using the pull test and the cross hatch test. The samples were on 1 mm thick soda lime glass.

a. Pull test. Adhesion was measured using a Positest Adhesion tester in accordance with standards ISO 4624 and ASTM D4541.[37,38] Aluminum dollies were fixed to the surface of the coating with an ethyl-2-cyanoacrylate based adhesive. The dollies were left to set and then loaded into the Positest adhesion tester and held firmly in place using a quick coupling mechanism. The Positest instrument was then used to apply a uniform and increasing force to remove the dolly from the surface of the coating. A stand-off is used to keep the substrate in place while the pull-off force is

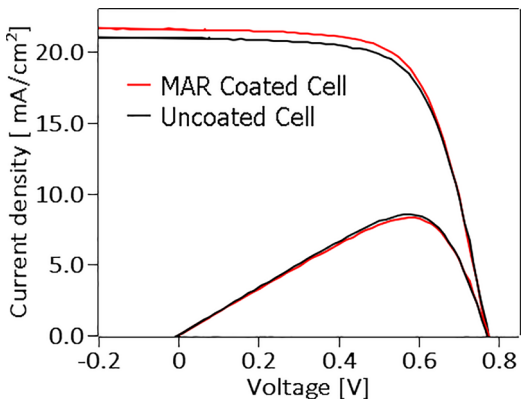

FIG. 6. (Color online) J-V characteristics of a CdTe solar cell at full sun illumination, before and after the application of a MAR coating.

TABLE II. Measured performance of MAR for CdTe.

	Layers	d (nm)	WAR (%)	FF (%)	J_{sc} (mA/cm^2)	Voc (mV)	Efficiency (%)
CdTe	0	0	4.22	65.6	20.98	774	10.55
	4	277	1.22	65.5	21.63 (+3.1%)	770	10.93 (+3.6% relative increase)

increased. A schematic diagram of the Positest is shown in Fig. 7. The load is increased at a steady rate until the coating fails and delaminates from the substrate.

Applying the pull test to the MAR coated surface failed to delaminate the coating from the surface of the glass. All experiments resulted in the glass substrate failing before the MAR coating delaminated, destroying the sample. Figure 8 shows the result of a test conducted with the highest recorded pull force of 0.98 MPa. This demonstrates that the MAR coatings have excellent adhesion. However, applying the pull test to thicker, and therefore stronger, MAR coated glass could reveal the true failure point of the coating.

b. Cross-hatch test. The standard test is to create a pattern consisting of six parallel lines by scratching the coating using a round, six bladed, steel cutting knife manufactured by Dyne Technology, Inc. (model number: CC1000). Then, six parallel lines are scratched, intercepting the initial lines at 90°, creating a cross-hatch pattern. However, the coating was too hard to be scratched by the standard round, six-bladed cutting knife, and a diamond scribe was used to scratch the samples instead. A semitransparent pressure sensitive tape (manufactured by q-connect) was then applied to the cross-hatched area and removed at a 90° angle from the surface of the coating, as quickly as possible. The coating was then assessed in accordance with ISO 9211-4.[4] The coating was given a rating between 0 and 5 based on observed delamination after the application and removal of tape. A score of 0 indicates excellent adhesion; a score of 5 indicates coating removal and extremely poor adhesion.

As shown in Fig. 9(b), the coatings showed very little damage after the application of tape: less than 5% of the total area was delaminated. However, some flaking can be observed at scratch intersections, and this is caused by the diamond scribing and not by the tape; thus, the coating has an adhesion rating nearing 0. This confirms that the MAR coating has excellent adhesion on glass. A full description of the classifications from the rating system is provided in the ISO 9211-4 specifications.

2. High temperature stability

Many processes in thin film CdTe solar cell manufacturing involve high temperatures, such as the CdTe deposition and the cadmium chloride ($CdCl_2$) activation treatment. It is likely that module manufacturers would prefer to source glass with the MAR coating already applied. This would provide the benefit of improved module efficiency without the need to include another process step or incur its associated capital expenditure. Glass companies are familiar with magnetron sputtering processes and there should be no technical barrier for coating glass directly from a float line. However, this strategy is only feasible if the precoated MAR coating on glass can withstand the subsequent high PV manufacturing process temperatures. MAR coated glass samples were heated to increasingly high temperatures to test the heat resistance of the coatings. Coatings on soda lime glass were heat treated at 100 °C intervals between 100 and 600 °C, at temperatures higher than this a low expansion coefficient Eagle Glass® was used.

The first signs of damage began to appear at 590 °C as small fissures became visible on the surface of the samples. The coatings had crazed uniformly at 600 °C. Figure 10(a) shows an optical image of a MAR coated sample which is undamaged after heat treatment at 580 °C, and Fig. 10(b) shows the coating has begun to craze uniformly at 600 °C.

The soda lime glass substrate had begun to warp in samples exposed to temperatures greater than 550 °C. Crazing is partly caused by mechanical stress from the warping glass substrate. To test the effect of the substrate on the crazing temperature of the coatings, samples on high temperature Eagle glass were prepared and heat treated at 100 °C

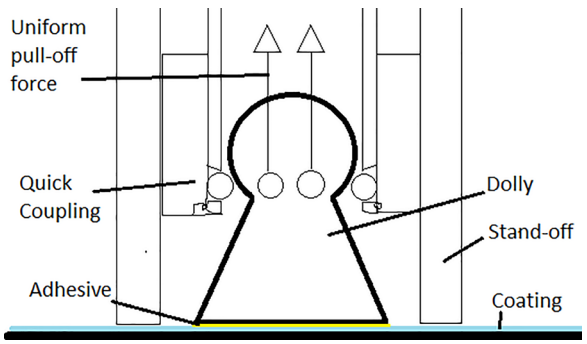

FIG. 7. (Color online) Schematic diagram of a dolly fixed to the coating surface using an adhesive, showing the dolly, stand-off, coupling, and uniform pull-off force lines.

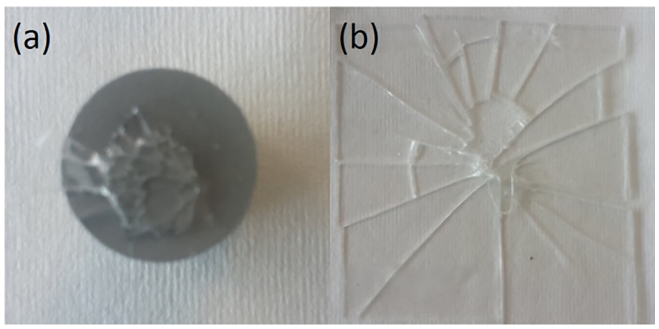

FIG. 8. (Color online) (a) Base of a dolly with glass adhered to the surface, indicating no coating delamination. (b) A fractured sample of an MAR coating on glass after a pull test. The coating remained undamaged.

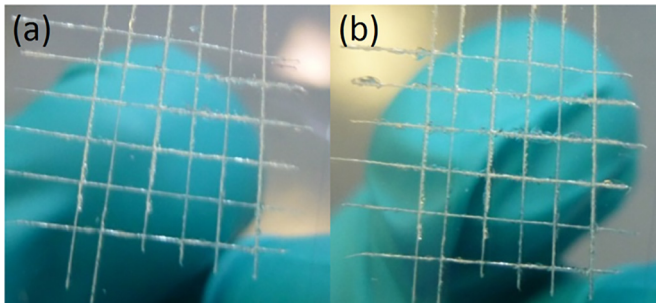

FIG. 9. (Color online) Cross-hatch test before (a) and after the application of tape (b).

intervals. The samples on Eagle glass survived up to temperatures of 800 °C, as shown in Fig. 11.

3. Resistance to temperature and humidity

Solar modules are used in many climates, some of which are particularly hot and humid such as occur in Equatorial regions. MAR coatings used on all solar cell technologies must be able to withstand high humidity, high temperatures, and temperature cycling.

A DH test was performed, in accordance with the IEC 61646 standard. The three samples were stressed in a Sanyo Gallenkamp HCC065 environmental chamber at 85 °C and

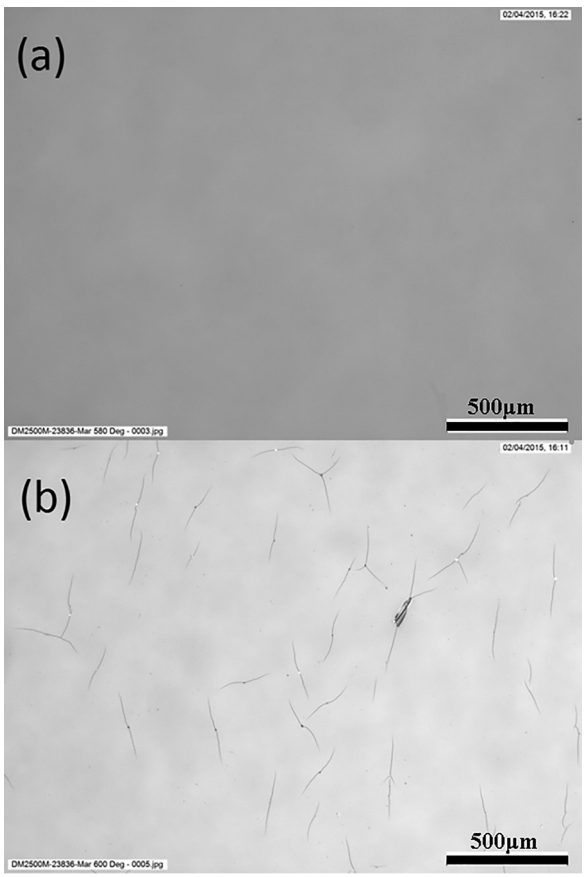

FIG. 10. (a) Optical microscope image of an MAR coated sample on soda lime glass exposed to 580 °C for 30 min, showing no visible crazing. (b) Optical microscope image of an MAR coated sample exposed to 600 °C for 30 min, revealing the occurrence of mild crazing.

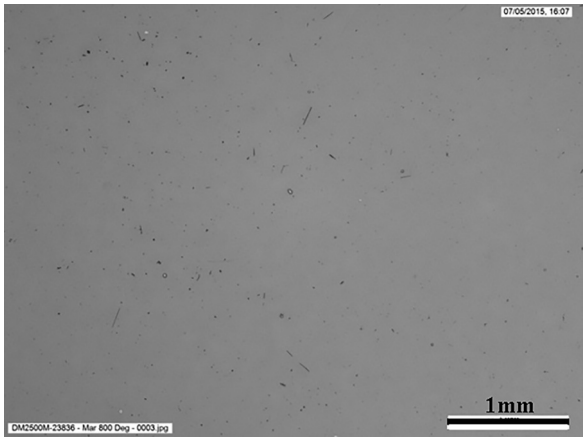

FIG. 11. Optical microscope image of an MAR coated sample deposited on high temperature Eagle glass and then exposed to 800 °C for 30 min, revealing mild crazing.

85% relative humidity for a total of 1000 h. Prior to the test, the samples were visually inspected, and reflectance measurements were taken. The samples were then taken from the chamber for testing at 20, 85, 160, 250, 325, 420, 500, and 1000 h. Figure 12 shows the measured WAR of the samples after each was exposed to damp heat up to 1000 h.

The WAR remained relatively constant after 1000 h of 85 °C/85% Damp Heat testing carried out in accordance with the IEC 61646 test for Photovoltaics devices. These accelerated tests show that humidity has a little effect on the coating stability and is unlikely to cause delamination or other damage in the field.

4. Stability against thermal cycling

Solar modules in the field will experience changing temperatures over 24 h due to the day/night cycle and the seasonal weather patterns. Accelerated lifetime testing of the MAR coatings was performed by cycling the MAR coatings at −40 to 85 °C in a Vötschtechnik VCS 7430-4H climatic chamber, with a minimum dwell time of 10 min at each temperature extreme. The WAR of the samples was then measured after 0, 100, 150, and 200 cycles. Figure 13 shows the WAR measured for three samples, which were cycled 200 times in accordance with the IEC 61646 protocol.

No coating degradation was observed as a result of the thermal cycling test, according to the IEC 61646 test for photovoltaic devices. This qualifies the coating for use on photovoltaic modules and provides confidence that the coating will not be damaged by the day/night cycle.

5. Water solubility testing

MAR coatings must be resistant to prolonged exposure to water. MAR coated glass surfaces were exposed to different tests to measure the coatings resistance to water, according to the ISO 9211-4:2012 protocol.[4] The standard test uses conditions of increasing severity. The least aggressive test involves immersion of the glass samples for 6 h in deionized (DI) water. DI water is defined as water with a resistivity

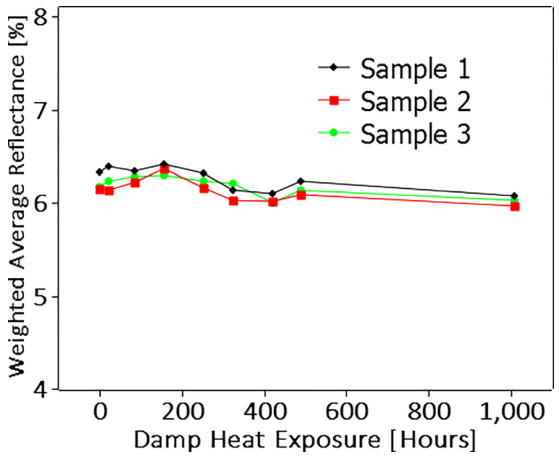

FIG. 12. (Color online) Measured weighted average reflectance (WAR) of samples after exposure to 85% humidity at a temperature of 85 °C, for up to 1000 h.

greater than 0.2 MΩ cm. This test is then extended to 24 and 96 h. Tests increase in severity to involve immersing the samples in boiling DI water for 5, 15, and 30 min. The most severe test involves submerging the sample in boiling DI water for 2 min, and moving it immediately into a bath of DI water at room temperature for 1 min. The tests were carried out using semiconductor grade DI water (18 MΩ cm resistivity). A sample was exposed to boiling DI water for 5, 15, and 30 min. The sample showed no sign of physical degradation. Figure 14 shows recorded WAR values obtained using a spectrophotometer.

The samples were then boiled again for 2 min and then placed in room temperature DI water for 1 min. According to ISO 9211-4:2012, this process constitutes a single test cycle. Ten cycles were applied to the sample, followed by visual inspection and spectrophotometer measurements. No changes were observed visually after each cycle. The WAR measurements are shown in Fig. 15. The samples passed the ISO 9211-4:2012 test with no sign of degradation. This result shows that MAR coatings can withstand wet climates and extreme weather.

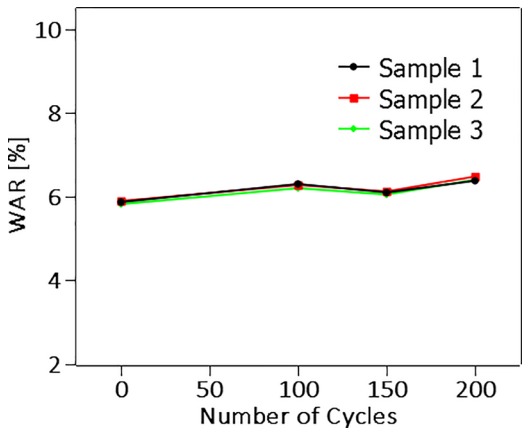

FIG. 13. (Color online) Measured weighted average reflectance (WAR) of MAR coatings cycled 200 times between −40 and 85 °C in a climatic chamber.

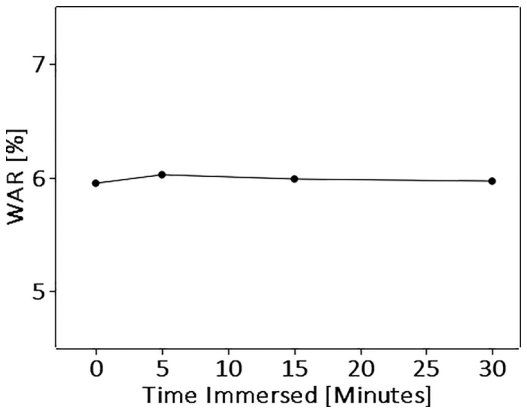

FIG. 14. Weighted average reflectance (WAR) of samples after immersion in boiling DI water.

6. Acid attack

Acid rain is common in many cities around the world. To test the acid resistance of the MAR coatings, samples were submerged in dilute sulfuric acid[39] with ∼3.5 *p*H. The type of acid and *p*H were selected to simulate acid rainwater.[40] The *p*H was measured using an Accumet AB150 *p*H meter. The WAR of the coating was measured after every 30 min of exposure. Figure 16 shows that the WAR of the coatings was not reduced after acid attack and demonstrates that the coating is resistant to acid rain.

7. Abrasion resistance

It is necessary for MAR coatings to be abrasion resistant to simulate the effect of transport, handling, maintenance, cleaning, and falling debris in certain environments. Abrasion resistance was measured using a reciprocating abraser adapted from BS EN 1096–2.[39] Materials such as cheesecloth[4] and felt pads[39] are used as abraders in industrial standards for optical coatings to simulate the effect of cleaning. A felt pad abrasion test from BS EN 1096-2 (which uses a slow turning circular abrader) was adapted into a linear abrasion test. In the adapted test, a felt abrader with a surface area of ∼7.5 mm^2 was applied to the surface of the MAR coating with a force of 10 N and passed across the surface

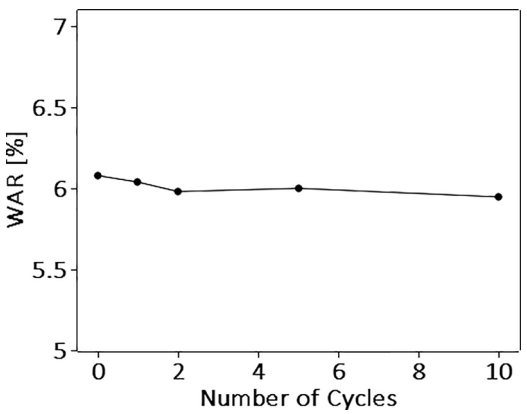

FIG. 15. Weighted average reflectance (WAR) of MAR coated glass after boiling water cycling.

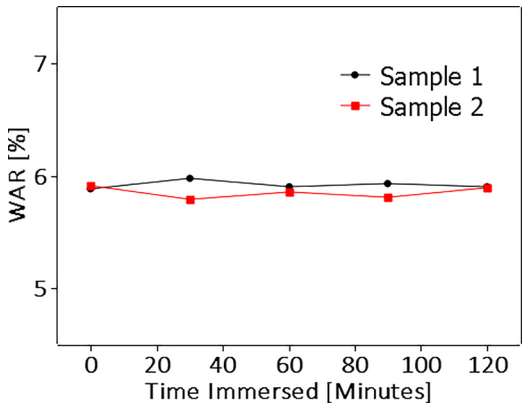

FIG. 16. (Color online) Weighted average reflectance (WAR) of MAR samples after exposure to dilute sulfuric acid simulating the effect of acid rain.

100 times, with a stroke length of 30 mm and a speed of 60 cycles per minute. Although more aggressive than the circular test found in BS EN 1096–2, the felt pad test caused no visible damage and had no effect on the WAR of MAR coated samples.

A CS-10 abrader,[41] a rubbery material with sand like grains within it, which produces a mild to medium abrasion, was used to further test the durability of MAR coatings. The CS-10 abrader was pressed to the surface of the MAR coated glass with a force of 5 and 10 N. The abrader was then repeatedly passed over the sample surface at 60 cycles per minute with a stroke length of 30 mm. After 100 cycles at each force, the coatings were cleaned in an ultrasonic bath and the WAR was measured.

After the abrader was applied to the surface of the MAR coating, the WAR was slightly reduced, by 0.2% and 0.4% for 5 and 10 N, respectively. The reduction in WAR is due to minor damage to the MAR coating. CS-10 abrasion is an aggressive test for optical coatings and the coating sustained only minor scratches. This demonstrated that the coatings can pass all industrial abrasion resistance standards for optical coatings and confirm the excellent durability of the MAR coatings

8. Scratch resistance

The scratch-resistance of the MAR coatings was measured using nanoindentation with a nanoscratch test.[42] The nanoscratch test is used to measure hardness using a diamond nanoindenter which is pressed into the surface of the sample using an increasing load. The surface of the sample then moves relative to the nanoindenter, scratching the surface. Recording the force at which the coating is penetrated deforms elastically and inelastically, and begins to flake, providing a quantitative measurement of the scratch-resistance of a coating. Additionally, images of the scratches provide qualitative evidence of the extent of the damage. For example, images show the size of flakes from the coating, and the size and number of fractures caused by the scratches.

A round end cone nanoindenter with a tip radius of 5 μm was used. Initially, the nanoindenter was held at a force of 0.1 mN at the surface of the sample. The load was then

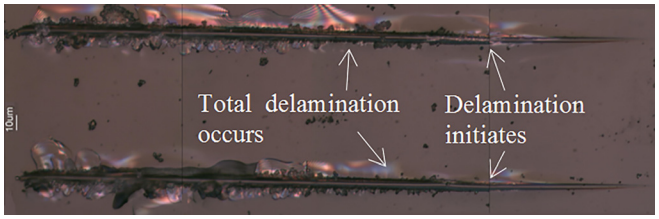

FIG. 17. (Color online) Scratches in the surface of an MAR coated sample. The scratches were produced by pressing a nanoindenter into the surface of the coating and moving the sample as the load is increased.

increased at a rate of 1 mN per 1 μm as the nanoindenter traveled across the surface. The nanoindenter traveled 400 μm and applied a maximum force of 400 mN over the 5 μm nanoindenter tip, ~5 kPa pressure.

An image of the resulting scratch from the nanoscratch test is shown in Fig. 17. The image shows that debris begins to appear next to the scratch at about ~120–140 mN: this is the point at which partial delamination of the sample begins to occur. This point on the scratch is indicated in Fig. 17 with a label reading "Delamination initiates." It is probable that the top layers of the coating failed, and the debris observed is likely to be from the top layers of the coating. At ~200–220 mN it appears that the debris from the coating is much larger and displays interference effects, which indicates that the coating has begun to delaminate as a whole rather than in layers. In Fig. 17, this point is indicated by the label reading "Total delamination occurs." There are no cracks protruding from the scratch and the flake size is very small. This confirms the coating is very hard and structurally sound.

The dependence of the penetration depth on applied load is shown in Fig. 18. Throughout the scratch process, the relationship between applied load and scratch depth remains linear, except for a few slight variations at the coating failure. This indicates that the resistance to deformation of the coating is similar to that of the glass substrate.

V. SUMMARY AND CONCLUSIONS

The increase in transmission using a four layer MAR coating has been shown to increase the light intensity

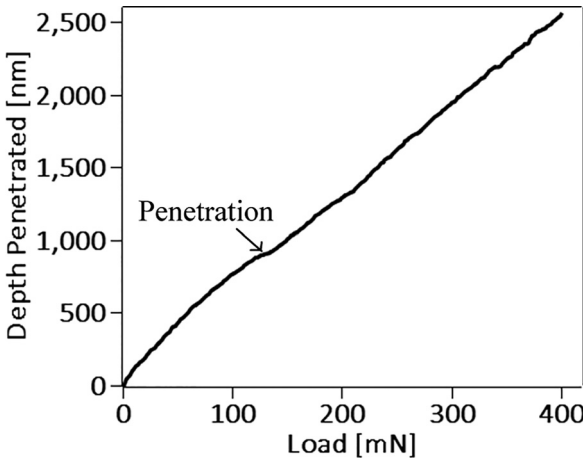

FIG. 18. Plot of the load applied to the nanoindenter against depth penetrated into the surface of the sample.

through the air–glass interface, resulting in an efficiency increase of 3.6% relative. The MAR coating used in this study reduced the WAR at the air–glass interface to just 1.22% across the 350–850 nm wavelength range, and increased the short circuit current density of CdTe cells by 3.1%. STEM imaging of a cross section of the coating confirms that techniques, such as reactive magnetron sputtering, provide sufficient practical control of layer thickness to achieve the antireflection effect predicted by the design. Coating uniformity is also excellent and easily technically achievable over typical module areas $>1\,m^2$.

The adhesion and durability of the coating is a primary concern. Solar modules are installed with a 25 year warranty even in countries with harsh climates. Not only is the coating expected to withstand humidity and temperature cycling, it may also endure dilute acid attack from atmospheric pollution. Furthermore, the coating must have sufficient scratch resistance to withstand regular cleaning and maintenance.

The adhesion of the MAR coatings has been tested using a battery of standardized tests. The pull test (ISO 4624) failed to remove the coating from the substrate, and the highest recorded pull strength that the coating survived was 0.98 MPa. This force failed to delaminate the coating, but destroyed the glass substrate. The cross-hatch test (ISO 9211-4) usually uses a four-bladed steel knife to scratch the samples, but had to be adapted to use a diamond tool to scratch the grid pattern into the coating. Very little delamination from the application and removal of tape was observed. In addition to these standard test methods, a nanoindentation scratch test was carried out on the MAR coatings. The nanoindentation scratch test shows that the coating has similar hardness to the glass substrate. The test also confirms the exceptional adhesion to the glass surface.

It may be cost-effective for MAR coatings used on solar modules to be readily available to PV manufacturers on precoated glass. This would be ideal for cover glass applications for crystalline silicon, thin film amorphous silicon, CIGS, CZTS, or perovskite devices. However, for this to be feasible for thin film CdTe devices using the conventional superstrate configuration, the coatings must be resistant to the temperature levels used at every stage of the thin film CdTe PV manufacturing process. This study has shown that the magnetron sputtered coatings are heat resistant and begin to craze at temperatures greater than those used both in the CdTe absorber deposition and activation processes ($\sim$500 °C). The first signs of crazing on soda lime glass were observed at 590 °C, as the glass substrate began to deform beneath the coating, applying mechanical stress. Applying the coating to Eagle glass (which has a lower coefficient of thermal expansion) confirms that the coating crazes once the underlying glass deforms at 800 °C. The WAR of the MAR coated surfaces was unaffected by heat treatment, even after crazing. The resistance of the MAR coatings to extreme heat makes its application and attractive for all PV technologies.

Temperature and humidity, thermal cycling, and acid attack tests resulted in no degradation of the MAR coating quality. This confirms that MAR coatings are suitable for use in any climate, tropical or otherwise, and are suitable even for use in areas of high ambient pollution.

This combination of tests demonstrates the remarkable robustness of MAR coatings. The 3.6% increase in relative conversion efficiency available by using precoated glass superstrates is also attractive. Its use would add a further $\sim$100 MW of capacity to the current $\sim$3 GW of thin film CdTe production without any physical modification to the manufacturing line. Neither would it affect the manufacturing time.

The cost of MAR coatings on cover glass or superstrate glass configurations could be reduced dramatically at high volumes. Although we have used planar magnetrons, it is feasible to use sputtering sources such as rotatable magnetrons with higher target utilization and deposition rates. These are used as standard in large scale industrial glass coaters.[43]

The dielectric metal-oxide multilayers used in MAR coatings have remarkable durability, adhesion, and resistance to environmental factors. Not only do they increase the power output of solar modules, their mechanical properties are consistent with a long warranty, even when exposed to regular cleaning cycles and maintenance.

ACKNOWLEDGMENTS

The authors are grateful to UKERC for funding this work through the EPSRC Supergen SuperSolar Hub (EP/J017361/1 and EP/M014797/1). One of the authors (G.W.) is grateful to NSIRC, Ltd., for supporting a CASE studentship. The authors are also grateful to W. Sampath and K. Barth of Colorado State University for the thin film CdTe cell used in Fig. 5.

[1]C. H. Chen, S. Y. Li, A. S. T. Chiang, A. T. Wu, and Y. S. Sun, Sol. Energy Mater. Sol. Cells **97**, 1694 (2011).
[2]G. Womack, P. M. Kaminski, and J. M. Walls, *42nd IEEE Photovoltaic Specialists Conference* (2015), pp. 2980–2986.
[3]C. R. Osterwald and T. J. McMahon, Prog. Photovoltaics **17**, 11 (2009).
[4]ISO 9211-4, *Optics, Photonics-Optical coatings, Part 4: Specific Test Methods* (ISO, 2012).
[5]L. Yan, N. Liu, S. Zhao, H. Yan, H. Lü, and X. Yuan, Acta Metall. Sin. **27**, 649 (2014).
[6]D. Chen, Sol. Energy Mater. Sol. Cells **68**, 313 (2001).
[7]P. M. Kaminski, F. Lisco, and J. M. Walls, IEEE J. Photovoltaics **4**, 452 (2014).
[8]P. M. Kaminski, G. Womack, and J. M. Walls, *40th IEEE Photovoltaic Specialists Conference* (2014), pp. 2778–2784.
[9]N. Sahouane and A. Zerga, Energy Procedia **44**, 118 (2014).
[10]G. Rajan *et al.*, *42nd IEEE Photovoltaic Specialists Conference* (2015), pp. 1506–1511.
[11]M. A. Green, K. Emery, Y. Hishikawa, W. Warta, and E. D. Dunlop, Prog. Photovoltaics **24**, 3 (2016).
[12]First Solar, *First Solar Achieves Efficiency, Durability Milestones* (Investor's Business Daily, Tempe, 2015).
[13]K. L. Barth, R. A. Enzenroth, and W. S. Sampath, *33rd IEEE Photovoltaic Specialists Conference* (2008), pp. 551–555.
[14]A. D. Compaan, A. Gupta, J. Drayton, S.-H. Lee, and S. Wang, Phys. Status Solidi **241**, 779 (2004).
[15]V. V. Plotinikov, C. W. Carter, J. M. Stayancho, N. R. Paudel, H. Mahabaduge, D. Kwon, C. R. Grice, and A. D. Compaan, *39th IEEE Photovoltaic Specialists Conference* (2013), pp. 405–408.
[16]J. P. Enriquez and X. Matthew, Sol. Energy Mater. Sol. Cells **81**, 363 (2003).
[17]J. M. Kephart, R. M. Geisthardt, and W. S. Sampath, Prog. Photovoltaics **23**, 1484 (2015).

[18]C. Rathweg, U.S. patent 8,207,006 (26 June 2012).
[19]R. Garabedian, R. Malik, J. Theil, J. Trivedi, and M. Yu, U.S. patent 0,040,970 (2 December 2015).
[20]S. Woo, S. Kim, and C. K. Hwangbo, J. Korean Phys. Soc. **45**, 1 (2004).
[21]P. K. Biswas, D. Kundu, and D. Ganguli, J. Mater. Sci. Lett. **8**, 1436 (1989).
[22]Azom, "Silica-silicon dioxide (SiO2)," 2001, http://www.azom.com/article.aspx?ArticleID=1114.
[23]J. F. Shackelford, Y.-H. Han, S. Kim, and S.-H. Kwon, *CRC Materials Science and Engineering Handbook*, 4th ed. (CRC Press, Boca Raton, 2015).
[24]Azom, "Zirconia–zirconium dioxide (ZrO2)," 2001, http://www.azom.com/article.aspx?ArticleID=133#_Key_Properties.
[25]P. Dahl, I. Kaus, Z. Zhao, M. Johnsson, M. Nygren, K. Wilk, T. Grande, and M. A. Einarsrud, Ceram. Int. **33**, 1603 (2007).
[26]E. P. Meagher and G. A. Lager, Can. Mineral. **17**, 77 (1979).
[27]A. R. Oganov and A. O. Lyakkhov, J. Superhard Mater. **32**, 143 (2010).
[28]W. Martienssen and H. Warlimont, *Springer Handbook of Condensed Matter and Materials Data* (Springer, Frankfurt, 2005).
[29]H. O. Pierson, *Handbook of Chemical Vapor Deposition: Principles, Technology and Applications* (Noyes/William Andrew, New York, 1992).
[30]Y. W. Bae, W. Y. Lee, and D. P. Stinton, J. Am. Ceram. Soc. **78**, 1297 (1995).
[31]A. Macleod and C. Clark, *Coating Design with the Essential Macleod* (Thin Film Center Inc, Tucson, 2012).
[32]G. Rajan, K. Aryal, T. Ashrafee, K. Shankar, A.-R. Ibdah, V. Ranjan, R. W. Collins, and S. Marsillac, *42nd IEEE Photovoltaic Specialists Conference* (2015), pp. 4–7.
[33]D. Ristau *et al.*, Appl. Opt. **41**, 3196 (2002).
[34]S. Schiller, U. Heisig, and K. Goedicke, J. Vac. Sci. Technol. **12**, 858 (1975).
[35]J. W. Seeser, P. M. LeFebvre, B. P. Hichwa, J. P. Lehan, S. F. Rowlands, and T. H. Allen, *35th Annual Technical Conference Proceedings of the Society of Vacuum Coaters* (1992), pp. 229–235.
[36]J. M. Walls, "Optical coatings for ophthalmic lenses by reactive magnetron sputtering," in *Optical Interface Coatings, Technical Digest 2001'* (Optical Society of America, Washington, 2001).
[37]ISO 4624, *Paints, Varnishes–Pull-Off Test for Adhesion* (ISO, 2002).
[38]ASTM D4541, *Standard Test Method for Pull-Off Strength of Coatings Using Portable Adhesion Testers* (ASTM, 2002).
[39]Bs En 1096–22012, Glass in Building. Coated Glass. Requirements and Test Methods for Class A, B and S Coatings (British Standards Institution, 2002).
[40]ASTM D7356/D735, *Standard Test Method for Accelerated Acid Etch Weathering of Automotive Clearcoats Using a Xenon-Arc Exposure Device* (ASTM, 2006).
[41]ASTM D1044-13, *Standard Test Method for Resistance of Transparent Plastics to Surface Abrasion* (ASTM, 2013).
[42]R. H. Kim *et al.*, Nat Commun. **5**, 3583 (2014).
[43]M. Vergöhl, D. Rademacher, and A. Pflug, Surf. Coat. Technol. **241**, 38 (2013).